DR. ALICIA MASTRETTA-YANES (Orcid ID : 0000-0003-2951-6353)

MR. ALEXANDER T XUE (Orcid ID : 0000-0003-1521-6448)

DR. BRENT EMERSON (Orcid ID : 0000-0003-4067-9858)

Article type   : Original Article

Long-term *in situ* persistence of biodiversity in tropical sky-islands revealed by landscape genomics

Alicia Mastretta-Yanes*[1], Alexander T. Xue[2,3], Alejandra Moreno-Letelier[4], Tove H. Jorgensen[5], Nadir Alvarez[6], Daniel Piñero[7] and Brent C. Emerson[8,9]

1. CONACYT - CONABIO. Comisión Nacional para el Conocimiento y Uso de la Biodiversidad, México, Liga Periférico — Insurgentes Sur, No. 4903, 14010, México, DF, México
2. Department of Biology, City College and Graduate Center of City University of New York, 160 Convent Avenue, MR 831, New York, NY, 10031, USA.
3. Department of Genetics, Rutgers University, 604 Allison Road, Piscataway, NJ 08854, USA.
4. Jardín Botánico, Instituto de Biología, Universidad Nacional Autónoma de México, México, DF, 04510, México
5. Department of Bioscience, Aarhus University, 8000 Aarhus C, Aarhus, Denmark.
6. Department of Ecology and Evolution, Biophore Building, University of Lausanne, 1015 Lausanne, Switzerland
7. Departamento de Ecología Evolutiva, Instituto de Ecología, Universidad Nacional Autónoma de México, México, DF, 04510, México.
8. Island Ecology and Evolution Research Group, Instituto de Productos Naturales y Agrobiología (IPNA-CSIC), C/Astrofísico Francisco Sánchez 3, 38206 La Laguna, Santa Cruz de Tenerife, Spain.
9. School of Biological Sciences, University of East Anglia, Norwich Research Park, Norwich NR4 7TJ, UK.

Corresponding author: Alicia Mastretta-Yanes

email: amastretta@conabio.gob.mx / a.mstt.yanes@gmail.com

Abstract

Tropical mountains are areas of high species richness and endemism. Two historical phenomena may have contributed to this: (1) fragmentation and isolation of habitats may have promoted the genetic differentiation of populations and increased the possibility of allopatric divergence and speciation, and; (2) the mountain areas may have allowed long-term population persistence during global climate fluctuations. These two phenomena have been studied using either species occurrence data or estimating species divergence times. However, only few studies have used intraspecific genetic data to analyse the mechanisms by which endemism may emerge at the microevolutionary scale. Here, we use landscape analysis of genomic SNP data sampled from two high-elevation plant species from an archipelago of tropical sky-islands (the Transmexican Volcanic Belt) to test for population genetic differentiation, synchronous demographic changes and habitat persistence. We show that genetic differentiation can be explained by the degree of glacial habitat connectivity among mountains, and that mountains have facilitated the persistence of populations throughout glacial/interglacial cycles. Our results support the ongoing role of tropical mountains as cradles for biodiversity by uncovering cryptic differentiation and limits to gene flow.

Introduction

Tropical mountains are biodiversity hotspots that tend to have more species than the lowlands surrounding them (Myers *et al.* 2000). Their levels of species richness are particularly high due to both the presence of species with broad distributions and aggregations of locally endemic species (Kruckeberg & Rabinowitz 1985; Jetz *et al.*

2004). Variation in contemporary environment may provide some explanation for regional variation in the richness of geographically wide-ranging species, but the high level of endemism present in tropical mountains exceeds predictions using macro-ecological variables alone (Jetz & Rahbek 2002; Rahbek *et al.* 2007). This excess may, however, be explained if analyses incorporate the history of species and their habitats (Jetz *et al.* 2004; Graham *et al.* 2006; Fjeldså *et al.* 2012). Such an integrative approach has lead to the suggestion that tropical mountains are rich in biodiversity because they promote both species differentiation and long-term (glacial-interglacial) population persistence (Fjeldså *et al.* 2012). This represents a new and exciting advance that calls for phylogenetic and phylogeographic data to further our understanding of the origin and maintenance of low-latitude mountain biodiversity.

The small surface area of high mountain regions and their geographic isolation leads to small and fragmented populations. Such a scenario is expected to favour allopatric speciation and hence the evolution of many new endemic taxa (Kessler 2002). Several studies confirm this expectation and it is the most commonly cited explanation for elevational patterns of endemism (Kessler 2002). Parapatric speciation may also occur, although it seems to be a less frequent phenomenon (Weir 2009; Cadena *et al.* 2011; Päckert *et al.* 2012). With regard to allowing population persistence through time, tropical mountains have been found to be areas of low climate change velocity, meaning they are areas where biodiversity can survive through periods of global climate fluctuation through small altitudinal shifts instead of long latitudinal movements (Loarie *et al.* 2009; Sandel *et al.* 2011). Areas of low climate change velocity thus allow for relatively long-term (glacial-interglacial) *in-situ* (within a close horizontal distance to where they exist today) population persistence, in contrast to the range shifts or extinctions that are inferred for higher latitudes and shallower orography (Hewitt 1996;

Sandel *et al.* 2011). Population persistence is meaningful for the accumulation of endemism because it leads to the local aggregation of endemic species over time (Fjeldså *et al.* 1999).

The allopatric speciation and long-term persistence hypotheses have been examined using species occurrence data (e.g. Sandel *et al.* 2011; Krömer *et al.* 2013) and, more recently, incorporating molecular data for the estimation of species divergence times (e.g. Smith *et al.* 2014). The scale of analysis ranges from coarse continental data (Rahbek *et al.* 2007; Sandel *et al.* 2011; Fjeldså *et al.* 2012) to more detailed analyses of specific mountain ranges such as the Andes (e.g. Fjeldså *et al.* 1999; Kessler 2002), the Himalayas (e.g. Päckert *et al.* 2012) and the Eastern Arc Mountains of Tanzania and Kenya (Fjeldså & Bowie 2008). Although these studies have included an evolutionary perspective by jointly analysing species ranges with phylogenetic data, there remains a need for intraspecific analyses of the mechanisms by which endemism may emerge at the microevolutionary scale.

We address this knowledge gap by examining population genetic differentiation and habitat persistence within high-altitude tropical mountains, using as a study area the highest mountains of the Trans-Mexican Volcanic Belt (TMVB, Fig. 1). We take a population level approach because it is expected that areas that facilitate population persistence over intraspecific (phylogeographic) timescales should, in the absence of further geological change, also be stable across interspecific (phylogenetic) timescales, such that regions of genetic endemism will eventually lead to regions of high species diversity (Hugall *et al.* 2002; Carnaval *et al.* 2009). Thus, examining population differentiation and long-term population persistence at the microevolutionary scale can contribute to the evolutionary understanding of tropical mountain biodiversity.

To analyse tropical montane taxa over a timescale consistent with population genetic process, we frame our hypotheses under the expectations of a sky-island dynamic for the TMVB (Toledo 1982; Mastretta-Yanes 2015a). The TMVB is an area that comprises an archipelago of sky-islands at ~19ºN where the highest stratovolcanoes (>3,000 masl) emerged during the last 1.5 Myr (Ferrari *et al.* 2012). Species with current range limits above 3,000 masl are expected to: (1) have been restricted to high-elevation refugia during the interglacial periods of the Pleistocene (such as the present), where divergence could be promoted by restricted gene flow; and (2) have extended ephemerally to lowlands during glacial periods, where the probability of genetic admixture would be increased (Toledo 1982; Mastretta-Yanes 2015a). Therefore, for the TVMB, population differentiation is expected to be a function of topographical variables. Demographically, this sky-island dynamic translates into cycles of population contraction (interglacial periods) and expansions (glacial periods), which should be temporally synchronous among the different mountains, assuming these climatic conditions resulted in a pervasive effect. If glacial-interglacial habitat persistence occurred within mountains that are isolated from each other over extended periods, populations would be expected to accumulate private genetic variation.

To test the above-mentioned expectations, we focus on two timberline-alpine grassland plant species of the TMVB for which we generated genomic SNP data, *Juniperus monticola* and *Berberis alpina*, and the glacial/interglacial distribution of their habitat type. We first examine the distribution of suitable conditions across sampled mountains through limited altitudinal range changes during glacial/interglacial stages. We then investigate if genetic differentiation can be explained by the degree of historical or contemporary habitat connectivity among mountains. Finally, we assess co-demographic change across populations within a comparative framework,. We then use

these data to evaluate the general hypothesis that long-term environmentally stable conditions for these ecosystems persisted *in situ* throughout glacial/interglacial cycles.

Methods

Study system and sampling

Juniperus monticola and *Berberis alpina* were chosen for analysis from an initial set of five species (including *Eryngium proteiflorum, Cirsium ehrenbergii* and *Pinus hartwegii*) that have broad distributions within the TMVB and are easily distinguished from related species in the field (Mastretta-Yanes 2014)*. Eryngium proteiflorum* and *C. ehrenbergii* were not chosen for analysis because they are not diploid, and *J. monticola* and *B. alpina* were chosen over *P. hartwegii* because the latter also extends to Northern Mexico and Central America*. Juniperus monticola* and *B. alpina* are both shrubs that grow from 3,300 to 4,200 metres above sea level (masl) on rocky formations from above the timberline and into alpine grasslands of the TMVB (Adams 2014; Mastretta-Yanes 2014). Both species can live from several decades to up to few hundreds of years (Francis 2004; Adams 2008). Their reproductive activity starts at an age of 4-7 years in the case of *Berberis* (Peterson 2003) and of 10-20 years in the case of *Juniperus* (Bonner 2008), with both species showing irregular heavy seed crops and seed dormancy (Francis 2004; Bonner 2008). Regarding dispersion, both species produce fleshy fruits and cones, which in other closely related species are dispersed by birds and small mammals (Adams 2008; Peterson 2003). Thus, while these species are not phylogenetically close at all, they have relatively similar life histories and dispersal abilities. They are closely related to *J. flaccida* and *B. moranensis*, which grow at lower altitudes (800-2,600 masl and 1,800-3,150 respectively).

Mountain peaks from >3,000 masl within the TMVB and nearby areas of the Altiplano Sur (AS) and the Sierra Madre Oriental (SMOr) were surveyed for *B. alpina* and *J. monticola* during September-October 2010 and April-May 2011 (Fig. 1). *Berberis alpina* was found in a total of six of the 17 locations surveyed, and *J. monticola* in 13, which represent their known distribution within the TMVB and the AS. Samples of the closely related species and outgroups *B. moranensis, B. trifolia, B. pallida, J. flaccida, J. zanonii* and *J. deppeana* were collected at lower elevations (~2,000-3,150 for *Berberis* and ~800-2,500 masl for *Juniperus*) of the TMVB and at northernmost localities of the SMOr and Sierra Madre Occidental (SMOcc) in October 2010 and 2012. Sampling was performed with SEMARNAT permission No. SGPA/DGGFS/712/2896/10. Herbarium specimens of *B. alpina, B. moranensis, J. flaccida* and *J. monticola* were prepared and deposited within the Herbario Nacional in Mexico City (MEXU) or within Herbario CIIDIR in Durango.

Molecular methods

Based on data from related species, the sampled *Berberis* species have an expected genome size between 0.50 and 1.83 Gbp (Rounsaville and Ranney, 2010), while the range is from 9-10 Gbp for the *Juniperus* species (Zonneveld 2012). For both taxa, ddRAD libraries were prepared using modified versions of protocols by Parchman et al. (2012) and Peterson et al. (2012). For *Berberis*, the enzyme pair EcoRI-HF and MseI was used, while for *Juniperus*, the rare cutter SbfI-HF was used instead of EcoRI-HF, thus allowing for a narrower subsampling of the larger Juniper genome. Samples were randomly divided into three (*Berberis*) or 10 (*Juniperus*) groups with a common sequencing index (ddRAD libraries hereafter). All *Berberis* and two *Juniperus* libraries were sequenced using single-end reads (100 bp long) in a separate lane of an Illumina

HiSeq2000, while two libraries were sequenced in a single lane for the rest of the *Juniperus* libraries. Further details on *Berberis* laboratory protocol and sequencing output are detailed in Mastretta-Yanes et al. (2015b). For *Juniperus* this information is available in Supporting Information 1.

The *Berberis* dataset consists of 75 individually tagged specimens of *B. alpina* and *B. moranensis* (6-10 per mountain, Table 1), three samples of each outgroup (*B. trifolia* and *B. pallida*) and 15 replicated samples, with at least one replicate per population or species. The *Juniperus* dataset consists of 137 individually tagged specimens of *J. monticola* (10 per mountain, Table 1), four of *J. flaccida,* one of *J. deppeana,* one of *J. zanonii,* 10 negative controls and 20 replicated samples, with at least one replicate per sampling locality or species (with the exception of *J. deppeana*).

Sequencing output, de novo *assembly and loci filtering of RAD data*

Complete details of *Berberis* sequencing output and quality filtering are available in Mastretta-Yanes *et al.* (2015c). Briefly, after demultiplexing and quality trimming of *Berberis* raw reads, final sequences were 84 bp long. *Juniperus* raw reads were demultiplexed and quality filtered using *Stacks* v. 1.17 by: (1) truncating final read length to 87; (2) removing any reads with an uncalled base; (3) discarding reads with low quality scores (score limit 22 to 28, depending on the library); (4) discarding reads that have been marked by Illumina's chastity filter as failing; (5) filtering adapter sequences, and; (6) rescuing tags (allowing a mismatch of one between barcodes). See Supporting Information 1 for full details on *Juniperus* bioinformatic pipeline.

Here we refer to a RAD-locus as a short DNA sequence produced by clustering together RAD-alleles; in turn, RAD-alleles differ from each other by a small number of SNPs in certain nucleotide positions (SNP-loci). Data were *de novo* assembled using the

software *Stacks* (Catchen *et al.* 2011, 2013). Data from *Berberis* had been previously assembled in *Stacks* v. 1.02 with the parameter values $m=3$, $M=2$, $N=4$, $n=3$, *max_locus_stacks*=3 and a SNP calling model with an upper bound of 0.05 (Mastretta-Yanes *et al.* 2015c). Stacks v. 1.17 was used for *Juniperus* with the parameter values $m=10$, $M=2$, $N=4$, $n=3$, *max_locus_stacks*=4 and default SNP calling model. These settings were chosen after testing a wide range of parameters as in Mastretta-Yanes *et al.* (2015c), and optimising the recovery of a large number of loci while reducing the SNP and RAD allele error rates (Supporting Information 1). After *de novo* assembly, the data were filtered to keep only those samples that had more than 50% and 35% of the mean number of loci per sample for *Berberis* and *Juniperus,* respectively (different percentages were used according to sample size), and only those loci present in at least 80% of *Berberis* samples and 70% of *Juniperus*. Putative paralogous loci of the *Berberis* dataset were filtered by identifying loci where the frequency of the major allele equalled $p=0.5$ in more than one population or species, as detailed in Mastretta-Yanes *et al.* (2014). For the *Juniperus* dataset the same procedure was followed, but with the following modifications in response to the larger sample size: (1) putative paralogous loci had to meet the extra condition of showing the deviations from Hardy-Weinberg Equilibrium (HWE) of $H_{obs} >0.9$, negative F_{IS} or $F_{IS}=1$, and (2) putative paralogous loci private to a single population of *J. monticola* were also excluded by identifying loci where $p=0.5$ in any single sampling location, present in more than three individuals of that population and showing deviations from HWE. To ameliorate the effect of missing data on population genetics statistics, RAD-loci that were present in several sampling locations but represented by only one individual in any given population were also filtered. These extra conditions were not performed in the *Berberis* dataset due to the small sample sizes for some locations. Replicates were used to estimate error rates for

both taxa as in Mastretta-Yanes *et al.* (2015c). For downstream analyses, only one sample for each replicate pair was used, along with all the remaining non-replicated samples. For both species, only the first SNP of each RAD-locus was used for the population genomic analyses described below (to control for linkage disequilibrium).

Considerably fewer loci were recovered in *Berberis pallida*, compared to the other *Berberis* species, which is likely explained by mutations affecting restriction enzyme cutting sites as a consequence of a distant evolutionary relationship with the other species in the study. This species was therefore excluded from further analyses.

Population genomic statistics and population differentiation

The *populations* program of *Stacks* was used to estimate the number of private alleles, the percentage of polymorphic loci, heterozygosity, π, and F_{IS} at each nucleotide position for each sampling location (mountain) of each species. Pairwise F_{ST} values were estimated, defining each sampling location as a population. SNP data was exported to PLINK format and analysed with custom R v. 2.15.1 (R. Core Team 2012) scripts.

Population structure was inferred using the software Admixture v1.3 (Alexander et al., 2009) and a PCA, which was performed with SNPSRelate (Zheng et al 2012). For both analyses, a subset of the data with loci present in at least 80% of the samples was used. Values of K ranging from one to seven in *Berberis* and one to 13 in *Juniperus* were assessed for the Admixture analysis*.* The value of K that exhibited the lowest cross-validation error was chosen for plotting.

Timberline-alpine grassland distribution of glacial and interglacial periods

The distribution of the habitat of *J. monticola* and *B. alpina* was modelled using confirmed data points of timberline-alpine grasslands of the TMVB. This "ecosystem approach" to species distribution modeling (SDM) is useful to examine the habitat

distribution of rare species across climate fluctuations (Graham *et al.* 2006). Although this approach has been shown to perform below average with respect to model sensitivity, it excelled in specificity statistics and robustness against extrapolations far beyond training data, suggesting that the ecosystem approach is well suited to reconstruct historical biogeography and glacial distributions (Roberts & Hamann 2012). Alpine grassland herbarium and fieldwork records were used as presence points and independent environmental variables were extracted from the 19 bioclimatic layers of Hijmans *et al.* (2005). The modeling was performed using Maxent v. 3.3.3k (Phillips *et al.* 2006) and the potential distribution of the timberline-alpine grassland was projected to the LGM using the bioclimatic layers obtained from CCSM and MIROC initiatives (Braconnot *et al.* 2007). Full details of the modelling are available in Supporting Information 2.

Landscape genomics analyses

To examine if genetic differentiation and endemism can be explained by the degree of historical spatial isolation among mountains we tested for isolation by resistance (IBR) *vs* isolation by distance (IBD). The approach is similar to studies where the influence of landscape features on population structure is investigated (e.g. McRae *et al.* 2008; Moore *et al.* 2011).

Resistance distances (McRae 2006) for the IBR tests were used to estimate the effective distance among sampling localities, using as a conductance grid (the reciprocal of the resistance) each of the 13 resistance surfaces described below. This method is based on circuit theory and considers multiple potential paths of least resistance between sampling points (McRae 2006), thus performing better than similar approaches such as least-cost path analysis (McRae & Beier 2007; Moore et al. 2011).

Mantel tests with 10,000 permutations were performed to test for IBR and IBD using the pairwise effective distances for each resistance surface and the pairwise F_{ST} matrices of genetic differentiation for each species. The genetic differentiation matrices were linearized using the formula for isolation by distance $F_{ST}/(1 - F_{ST})$ as advocated by Rousset (1997). Subsequently, partial Mantel tests with 1,000 permutations were performed partialling out the flat resistance distances. Tests were carried out independently for both species and also for a subset of *J. monticola* populations (excluding Nevado de Colima and Tancítaro, see discussion). Analyses and graphical representations of data were performed with R using the packages *ape* (Paradis *et al.* 2004), *vegan* (Oksanen *et al* 2016), *ade4* (Dray & Dufour, 2007) and *ggplot2* (Wickham & Chang 2013).

The 13 resistance surfaces used here were based on: (i) environmental modelling ("present", "CCSM" and "MIROC" for the LGM); (ii) a "flat" landscape, and; (iii) elevation data (above 1800, 2000, 2300, 2500, 2700, 3000, 3300, 3500 and 4000 masl; Fig. 2). The 'flat' landscape surface is equivalent to testing for IBD using Euclidean distances, but it takes into account the fact that the underlying landscape is bounded and not infinite (Lee-Yaw *et al.* 2009; Moore *et al.* 2011). Resistance distances were estimated using the pairwise mode of the program *Circuitscape* v. 3.5.8 (McRae 2006; McRae & Beier 2007) setting the sampling locations as focal points. See Supporting Information 2 for further details. The suitable area in a 30 km radius was measured for each mountain for the ccsm, present, 3000 and 4000 resistance surfaces.

Comparative demographic inference using the aggregate site frequency spectrum

We tested which demographic syndrome (population expansion, contraction or constant size) best fits the history of each sampled mountain locality for both species, and then examined if the inferred demographic changes were synchronous. Each

mountain was considered an independent population with the aim of examining the role of the mountains themselves on co-demography through time.

We used the program *Multi-DICE* for comparative co-demographic inference of independent populations within a unified analysis (Xue & Hickerson, 2017). This method exploits the aggregate site frequency spectrum (aSFS), which is a summary statistic vector that contains signal of co-demographic population size changes and is assembled via a re-ordering procedure applied to genomic-scale data across independent populations in the form of the site frequency spectrum (SFS) (Xue and Hickerson, 2015; see Prates *et al* 2016 for an applied example). The aSFS can be coupled with an inferential framework to compare observed data with simulations generated under a hierarchical co-demographic model that freely hyperparameterizes degree of synchronicity (Xue & Hickerson, 2015, 2017, Prates et al 2016). Three main steps were applied to perform this analysis:

a. Downprojecting SNP data to equal sampling size. Since the aSFS assumes independence among populations as well as all requiring populations to be sampled for the same number of individuals, we re-performed SNP calling on each population individually, which minimized the amount of missing data and thus maximized the number of SNPs within each population (Xue and Hickerson 2015, 2017; Prates et al. 2016). Since there exists a trade-off among SFS sampling projections between more individuals and less applicable populations, as well as accommodating a higher number of sampled individuals versus a lower number of SNPs due to missing data (though the opposite relationship is the case with a low number of individuals due to an increase of monomorphic sites at lower sampling projections), two downprojected datasets that allow for alternative numbers of individuals per population were constructed. This was achieved by running the *populations* program of Stacks to export SNPs in order to keep

loci that were present in a minimum of four and five individuals per population (*-r* flag), respectively. The SNP data of each population were then down-projected using *dadi* 1.7 (Gutenkunst *et al.* 2009) to an SFS with sampling size of four and five, respectively.

b. Performing independent single population demographic analyses. *Fastsimcoal* version 2.5 (Excoffier *et al.* 2013) with the FREQ setting was used to directly generate 100,000 folded SFS simulations per model of instantaneous expansion, instantaneous contraction, and constant size for a total of 300,000 simulations, per each of the two down-projection datasets. Each SFS was simulated under 1,000 genealogies, which is based on the average number of SNPs across all the empirical SFS, and the following priors: time of size change $\tau \sim U\{1,000, 250,000\}$ generations ago; magnitude of size change $\varepsilon \sim U(0.02, 0.20)$ for expansion model and $\sim 1/U(0.02, 0.20)$ for contraction model; effective population size $N_e \sim U\{100,000, 2,000,000\}$ for expansion model, $\sim U\{50,000, 500,000\}$ for constant size model and $\sim U\{5,000, 100,000\}$ for contraction model. To clarify, these distributions were selected in the interest of discriminating general demographic syndromes as well as broadly encompassing all populations within the dataset, particularly for the downstream unified comparative analysis employing hierarchical co-demographic modeling (see following step c.), and not necessarily for thorough parameter estimation per every population. Following the simulations an approximate Bayesian computation (ABC) was done using the R package *abc* (Csilléry *et al.* 2012) o to infer demographic syndrome, as well as to estimate posterior distributions for time, magnitude of population size change and effective population size. Median and mode statistics of posterior distributions were calculated for point estimates. Simple rejection was performed with a tolerance level of 0.005.

c. Unified comparative analysis based on the aSFS. The results of the single population analyses were used to inform a multi-population co-demographic analysis, for which there were 10 expanders and four contractors (total of $n = 14$ populations) for the data down-projected to four individuals, and eight expanders and four contractors (total of $n = 12$ populations) for the data down-projected to five individuals. To clarify, a single analysis was performed per data projection that combined expanders together with contractors, as there is no strong indication that these demographic trajectories were in response to differing environmental conditions, either from the single population results nor from existing literature. Additionally, the much lower number of contractors would result in drastically reduced accuracy as well as utility in estimating hyperparameter values with the aSFS if analyses were categorised by demographic syndrome.

The priors for the SFS simulation were set to: time of size change $\sim U\{100,000, 2,000,000\}$ generations ago with a pulse buffer on the prior $\beta = 20,000$ generations (forcing all other time draws to be $> 20,000$ generations apart from each synchronous pulse timing; Xue & Hickerson, 2017), magnitude of size change $\sim U(0.05, 0.20)$ for expansion model and $\sim 1/U(0.05, 0.20)$ for contraction model, and effective population size $\sim U\{50,000, 500,000\}$ for expansion model and $\sim U\{5,000, 100,000\}$ for contraction model. Notably, the range for the time prior here is significantly widened with respect to the single population analysis in the interest of accommodating a wide range of potential co-demographic temporal scenarios (i.e. from idiosyncrasy to synchrony). Importantly, both *B. alpina* and *J. monticola* have a reproductive system of overlapping generations coupled with long lived reproductive individuals (Peterson 2003; Francis 2004; Adams 2008; Bonner 2008), compromising the accuracy for absolute estimation of time. While this could be addressed with translating number of generations into time

via weighing individuals by their reproductive value (Felsenstein 1971), this is not feasible for our species. Furthermore, without reliable information regarding mutation rate nor effective population size, there is no solid foundation for calibrating the time parameter (Xue and Hickerson 2017). However, given that each population experiences comparable habitat conditions (i.e. sky islands of approximately equivalent size) as well as belongs to one of two species with similar life histories and growth forms, it is not unreasonable to assume that the same effective population size prior can be applied universally across all populations. Therefore, time estimates, which are based on effective population size values within this coalescent framework, are directly comparable and in turn hyperparameter inference can be achieved.

Per dataset (i.e. down-projections to four and five individuals), two reference tables were constructed, each with a different hyperparameterization scheme. Following Xue & Hickerson (2017), the two hyperparameterization schemes included: (1) restricting synchrony to only a single pulse and varying the proportion of taxa having membership within this pulse $\zeta \sim U\{1, n\}/n$, with the remaining taxa temporally idiosyncratic in size change (the case of $\zeta = 1/n$ would represent total idiosyncrasy); (2) distributing taxa equally across synchronous pulses, the number of which is varied $\psi \sim U\{0, 3\}$, thus allowing no idiosyncratic taxa except in the case of total idiosyncrasy ($\psi = 0$). To clarify, for the latter scenario, when n is not divisible by the number of pulses, the remainder is distributed randomly across as many pulses as possible (*e.g.* if $n = 14$ and $\psi = 3$, then a random two of the three pulses would have five taxa and the remaining would have four taxa). This model simplification allows more accuracy in searching hyperparameter space while still providing co-demographic insight that supplements ζ inference, following the strategy outlined in Xue and Hickerson (2017). To construct each of the four total reference tables, 1,000,000 folded aSFS were simulated, with each

aSFS partitioned between the expanders and contractors such that the SFS simulated under expansion and the SFS simulated under contraction were each separately converted to two aSFS vectors, which were then concatenated (Prates *et al.* 2016; Xue & Hickerson, 2017). Each per-population SFS was simulated under 1000 genealogies using the priors mentioned before.

Hierarchical Random Forest (hRF) was performed for each reference table using the R package *randomForest* (Liaw & Wiener, 2002) and hierarchical ABC (hABC) was performed using the R package *abc*. To conduct hRF, we used 100 iterations of randomly selecting 5,000 simulations from the reference table to produce 10 decision trees, with the default 33% of variables per decision tree node. Decision trees were built to capture variation in ζ for the first hyperparameterization scheme and ψ for the second hyperparameterization scheme, and exploited for prediction of respective hyperparameter values from the empirical data using the R function *predict()*. To conduct hABC, simple rejection was performed with a tolerance level of 0.0015. The function *abc()* was deployed for hyperparameter estimation and parameter summary estimation of dispersion index (variance/mean) Ω and mean for timings of demographic changes across populations (with lower values signaling greater synchronicity). Median and mode statistics of posterior distributions were calculated for point estimates. For both hRF and hABC, "leave-one-out" cross-validation, which involves removing a simulation and treating it as a pseudo-observed dataset (POD) for estimation against the remaining reference table, was performed using the function *cv4abc* following the same specifications with 50 total PODs per reference table. Estimated values were leveraged against true POD values to calculate Pearson's correlation *r* and root mean squared error.

Results

Alpine grassland distribution during glacial/interglacial stages

The uncorrelated environmental variables selected for the timberline-alpine grassland modelling were isothermality, mean temperature annual range, temperature in the wettest quarter, precipitation seasonality and precipitation in the coldest quarter (Fig. 3a). For the present conditions (Fig. 3b), our modelling is congruent with the known distribution of the timberline-alpine grasslands in this region (Rzedowski 1978; Calderón de Rzedowski & Rzedowski 2005), but it may represent a slight overestimate (see Supporting Information 2 for discussion). The projection to the LGM shows that this ecosystem occurred in the same geographic areas, but with a larger distribution extending to lower elevations (Fig. 3b).

RAD-seq data yield

Berberis data used here correspond to the subset of "putative orthologs within *B. alpina*" described in Mastretta-Yanes *et al.* (2014). The dataset contains 3,669 SNPs (considering only the first SNP of each RAD-locus) with an error rate of 2.3% (SD 0.27), 19% missing data and a mean coverage of 10.3 (SD 4.6). For the *Juniperus* data (only *J. monticola* ingroup), 2,925 SNPs (considering only the first SNP of each RAD-locus) were recovered, with a SNP error rate of 1.4% (SD 0.8),16% of missing data and a mean coverage of 84.60 (SD 50.06).

Population genomic statistics and population differentiation

Populations from both species show private alleles ranging from 154 to 1101 and an average nucleotide diversity (π) ranging from 0.08 to 0.13 (Table 1). F_{IS} decreases from east to west for *Berberis* and shows no clear pattern in *Juniperus*, with values for F_{IS} from

0.03 to 0.07 (Table 1). Pairwise F_{ST} values for *B. alpina* populations ranged from 0.056 to 0.123 and all comparisons were significant, with the Cofre de Perote population showing the highest levels of differentiation and Tlaloc the smallest, relative to other populations (Table S2.1). For *J. monticola* pairwise F_{ST} ranged from 0.022 to 0.074 and all comparisons were significant, with La Malinche population showing the highest values of differentiation relative to other populations, and Tlaloc the smallest (Table S2.2).

The Admixture analyses of *B. alpina* returned a value of six as most optimal for K (Fig. S2.2a). The six groups broadly correspond to each mountain, but with some admixture between the westernmost populations (To-Aj) and among the central populations (Aj, Iz, Tl). The first four components of the PCA (Fig. S2.3a) explain 42.7% of the variance and reflect the same structure as the Admixture analysis. *Juniperus monticola* showed less structure, with K=3 (Fig. S2.2b) and 16.7% of the variance explained (Fig. S2.3b). Individuals from the west (Co, Ta) and east (Ci, Ne, Pe) form two groups that present some admixture with a third group composed of the remaining populations. Admixture within the third group is most pronounced within its eastern (Ma) and western (Bl) extremes.

Isolation by resistance

The resistance surface plots reveal that although most sampling locations are separated by comparable horizontal distances, there are important differences regarding the connectivity among locations, and these depend upon the elevation or distribution model used to set the conductance values (Fig. 2).

The Mantel and partial Mantel tests yielded positive significant results with different explanatory power depending on the surface used. The 'flat' landscape (i.e. IBD) was outperformed by some of the scenarios considering the environmental modelling or the elevation grids (Table 2). For *B. alpina* the highest explanatory power was provided by the resistance surface of 3,000 masl both for the Mantel ($r = 0.940$, p < 0.01; Table 2), and the partial Mantel test ($r = 0.717$, p < 0.05). For *J. monticola,* considering all populations, the surface with the highest explanatory power was the flat surface (Mantel $r = 0.499$, p < 0.05) and no partial Mantel test was significant. However, when excluding the populations of Nevado de Colima and Tancítaro, environmental modelling for the LGM using the CCSM layers provided the highest explanatory power both for the Mantel ($r = 0.686$, p < 0.001) and partial Mantel test ($r = 0.453$, p < 0.01).

Comparative demographic inferences using the aggregate site frequency spectrum

A high degree of temporal synchrony among population size changes in both species was detected across both single population and multi-population analyses and both sampling levels. The single population analyses (Table S2.3) showed that 10 populations are consistent with population expansion (*Berberis* Aj, Iz, Ma, TI, *Juniperus* Aj, Bl, Ch, Iz, Ne, Tl; population codes as in Fig. 1, see Supplementary Materials 2 for details on each population inference), four are consistent with contraction (*Berberis* To, *Juniperus* Co, Ma, To), two are consistent with constant size (*Juniperus* Ta, *Berberis* Pe) and two are inconclusive though largely consistent with constant size (*Juniperus* Ci, Pp). The estimates for the respective times of expansions and contractions (Table S2.3) appeared qualitatively similar overall (expansions median = 183,549-203,767 and mode = 224,859-232,145 generations ago; contractions median = 163,888-182,777 and mode = 215,792-228,586 generations ago) and the magnitudes (ancient/present

population size; Table S2.3) of size change were moderate as well as relatively similar in value across both population expansions (median = 0.115-0.126, mode = 0.139-0.178) and contractions value (median = 8.749-10.537, mode = 8.749-10.537; consider that the factor of expansion is the inverse of the magnitude). For the aSFS-based co-demographic analysis, across both hRF and hABC approaches and both sampling down-projections, there was an inference of low variability in the distribution of expansion and contraction times based on the Ω estimates (median Ω for uniform ζ distribution = 28,888 and 52,317, for four and five individuals, respectively) as well as a high proportion of populations within a single synchronous co-demographic pulse (hABC median ζ = 0.929 and 0.917, for four and five individuals, respectively), indicating a high degree of synchronicity (Tables 3, S2.4-5).

Discussion

We tested for population genetic differentiation and habitat persistence within the TMVB, by coupling species distribution modelling for glacial/interglacial cycles, landscape genomic analyses with explicit quantitative hypotheses, and analyses of demographic history within a comparative framework. These complementary sources of evidence support the hypothesis that tropical mountains have facilitated the differentiation and *in situ* persistence of alpine-grasslands species from the TVMB during the climate fluctuations of the Pleistocene.

Altitudinal changes of alpine grasslands

Ecosystem distribution modelling reveals that the alpine grasslands shifted altitude during the Pleistocene climate fluctuations, but would have persisted within some mountains during both glacial and interglacial periods (Fig. 3). It is important to note

that both our modelling approach and the available palynological and geological data are not species specific, and taxa may respond differently to subtle environmental differences or have different tolerance thresholds (Araújo & Guisan 2006; Roberts & Hamann 2012). Nonetheless, broadly speaking, the present and past distributions of timberline-alpine taxa from the TMVB are highly dependent on temperature or temperature associated variables, which in turn are highly correlated to altitude (Beaman 1962; Lauer 1978; Almeida-Leñero, *et al.* 2007). Thus, it is expected that the altitude of the landscape separating the highest peaks of the TMVB would play a key role in population isolation.

The modelled lower elevations of TMVB timberline-alpine grasslands during the LGM (Fig. 3c) is congruent with fossil pollen records down to 2,300-2,500 masl for reduced forests (similar to open forests close to the timberline) and grasslands (Lozano-García & Ortega-Guerrero 1994, 1998; Lozano-García *et al.* 2005; Caballero-Rodríguez et al. 2017). Moraines also reveal that snow lines dropped by approximately 1,000 m during glacial periods (Lozano-García & Vázquez-Selem 2005; Vázquez-Selem & Heine 2011). Considered together, the palynological, geological and niche modelling data all suggest that open forests and grasslands could have extended down to 2,300-2,500 masl at the LGM, and that suitable conditions for alpine vegetation (now at around 4,000 masl) could have been present at 3,000-3,300 masl.

Within the higher stratovolcanoes that reach more than 3,500 masl, altitudinal shifts of approximately 1,000 m can be achieved within a relatively short horizontal distance (3-6 km). This means that the alpine grasslands will shift altitudinally during glacial and interglacial periods, but with only limited horizontal displacement in the highest mountains. When such mountains are flanked by lower altitude terrains, forests

are expected to both remain isolated and persistent locally over timescales exceeding the periodicity of a glacial cycle (Fig. 3b-c).

Glacial distribution explains population differentiation

Populations of both *J. monticola* and *B. alpina* are genetically structured. Structure is more marked in *Berberis,* which could be expected given the limited number of highly isolated mountains where it was found. However, in both species the western and eastern populations are more differentiated than populations within the central part of their distributions, which presented more admixture (Figs. S2.2 and S2.3). These central populations correspond to the part of the TMVB where topography facilitates connectivity among the sampled mountains (Fig. 2), suggesting a role for landscape driving population differentiation.

Testing for IBR using surfaces that consider present and past potential habitat distributions shows that, as predicted, accounting for topography-driven connectivity better explains population differentiation than simple geographic distance (Table 2). The population genetic differentiation of both species was better explained by resistance surfaces likely representing their glacial distributions (~1,000 m below the elevation where they are currently more abundant). This result is not surprising when considering that: (1) the timberline attained its present altitude only 3,000 yr ago (Lozano-García & Vázquez-Selem 2005); (2) the last 700,000 yr have been dominated by major glacial periods with a ~100,000 yr cycle interrupted by relatively short warm interglacials (Webb & Bartlein 1992); so that (3) recent distributions could be considered a perturbation of the "historical average", and (4) *Berberis* and *Juniperus* are slow growing and long lived, such that the number of generations representing the present distribution could be relatively small.

For *B. alpina,* the explanatory power was highest in the IBR test with the surface allowing for connectivity at 3,000 masl both in the Mantel test ($r = 0.940$) and the partial Mantel test ($r = 0.717$, $p < 0.05$). This indicates that although simple geographic distance provides explanatory power, more of the variance is explained if connectivity through time is considered (Fig. 4). This also holds for *J. monticola*, when Nevado de Colima and Tancítaro populations were excluded from the analysis (Fig. 5), as the IBR test with the LGM-CCSM surface held more explanatory power (Mantel $r = 0.686$, $p < 0.001$, and partial Mantel $r = 0.452$, $p < 0.01$; Table 2) than the other surfaces. The Nevado de Colima and Tancítaro mountains are considerably further away from the remaining high mountains of the TMVB (Fig. 1). Importantly however, our models infer that they were not connected by alpine grasslands to the Central TMVB during the Pleistocene glaciations. They remained isolated in both LGM models, even when allowing connectivity at altitudes as low as 2,300 masl (Fig. 2). These populations were thus more likely to have been founded by long distance colonisation, as opposed to climate mediated gene flow with other populations.

Results for both species are consistent with population differentiation being influenced by the landscape matrix among mountain peaks, and historical habitat connectivity patterns associated with this. In particular, the connectivity that occurred during the likely glacial distribution of each species. This fits the prediction of gene flow occurring at higher rates during glacial periods. The importance of the topographic matrix connecting mountains is noteworthy, as even during their glacial extension species seem to have maintained a fragmented (island-like) distribution (Fig. 2). Therefore glacial admixture is expected to have occurred more readily among certain population clusters (e.g. Tláloc-Iztaccihuatl-Popocatepetl, Fig. 2), while other populations should have remained isolated during interglacial stages. This is also

supported by the Admixture (Fig. S2.2) and PCA (Fig. S2.3) analyses that reveal distinct groups for the more topographically isolated populations, and more shared ancestry and gene flow among populations inferred to have higher connectivity during the glacial stages (e.g Aj, Pp, Iz, Tl, Fig. 2).

Population differentiation and persistence under a sky-island dynamic

Our analyses of historical habitat distribution, together with genetic differentiation and co-demographic history of two high altitude plant species, support a sky-island dynamic within the TMVB that has promoted population differentiation and long-term *in-situ* persistence. Niche modelling demonstrates that since their emergence during the last 1.5 Myr (Ferrari *et al.* 2012), the highest volcanoes of the TMVB have provided stable conditions throughout glacial-interglacial cycles suitable for continuous population persistence for subalpine and alpine taxa.

The genetic data supports a scenario of long-term population persistence in both species. Genomic differentiation was significant among all populations, with F_{ST} values typically greater than 0.05 (Table S2.1 and S2.2), which is congruent with populations diverging in allele frequencies and accumulating private alleles through the effects of genetic drift and mutation, and reduced amounts of gene flow (Table 1). Geographic structuring of genetic variation was found for both species (Fig. S2.2 and S2.3), with genetic groups matching the levels of glacial connectivity expected from topographic variables.

In addition to differentiation, a demographic syndrome of either moderate (expansion and contraction magnitudes ~ 9x) population expansion or constant size was inferred for most populations of both species (Table S2.3). These magnitudes are close to the lower end of the prior used (5), which is as far as low that can be detected

by this analysis. Therefore, although some demographic change was detected, this is close to population size constancy or limited size fluctuations. This demographic history of relative stability is consistent with a sky-islands scenario for the TVBM for two reasons. First, suitable habitat is expected to have persisted in situ within the TMVB for both focal species during climate fluctuations (Fig. 3), thus allowing for *in situ* population persistence. Second, estimated glacial ranges are not much larger than interglacial ranges, which predicts only limited population size change through a glacial cycle. For instance, the ccsm suitable area is around 1x times larger than the present area, and the suitable area above 3,000 masl is 12x times larger than the suitable area above 4,000 (Fig. 2). More substantial demographic change is expected for species from lower altitudes of the Mexican highlands (Mastretta-Yanes *et al.* 2015a), and for taxa with more northern distributions (Hewitt 1996; Stewart *et al.* 2010), where species contracted or expanded across large horizontal distances (e.g. continental Europe) during the Last Glacial Maxima to the present.

Although we could not estimate the absolute timing of these demographic events, we can infer that they occurred synchronously among populations of both species (Table 3). Importantly, our co-demographic model did not account for genetic variation from shared ancestry or migration, which could have potentially contributed to the detected signal if such events coincided with the inferred synchronous co-demographic size changes (Xue and Hickerson 2017). Given the relatively old time of synchronous pulse (~300,000 generations ago) inferred by the aSFS analyses, the demographic signal detected could be related to the founding event following sky-islands colonization. But if such were the case, it would imply that no demographic

change strong enough to erase this signal occurred since then, which is consistent with a co-demographic history of relative population stability and persistence within sky islands.

Conservation and management implications

Most of the sampled mountains of this study are Natural Protected Areas (NPA) currently under different threats and management methods. Our results highlight the conservation value of the TMVB peaks, showing that they are areas of long-term biodiversity persistence despite historical climate fluctuations. Our results are also relevant for the management of these NPA. Firstly, because we show that these mountain peaks behave like islands showing high levels of genetic isolation. As a consequence, we suggest that these mountains should be managed like islands, for instance promoting the use of native germplasm for reforestation efforts. Secondly, our results show that alpine grasslands from the TMVB are a natural ecosystem that has historically persisted within these mountains. Therefore the aforestation of these grasslands, as currently done in some of the mountains, is destroying a natural ecosystem of conservation importance.

Conclusion

We have shown with different sources of evidence that: (1) the highest stratovolcanoes of the TMVB facilitated the existence of timberline-alpine grasslands throughout glacial/interglacial cycles (long-term *in situ* population persistence); and (2) population genetic differentiation of species from this ecosystem can be explained by the degree of habitat connectivity among mountains during the glacial periods.

Similar scenarios have been postulated for taxa of the TMVB from lower altitudes using classical population genetic and phylogeographic approaches (e.g. McCormack *et al.* 2008; Bryson *et al.* 2011, 2012; Gutiérrez-Rodríguez *et al.* 2011; Ornelas *et al.* 2013; Parra-Olea *et al.* 2012). Some of these previous phylogeographic studies focusing on divergence times (e.g. Ornelas *et al.* 2010; Bryson *et al.* 2012a; b; Leaché *et al.* 2013) have not been able to distinguish between the confounding effects of climate and geological change, because in the TMVB climate fluctuations and volcanic changes co-occurred during the Pleistocene (Mastretta-Yanes et al. 2015). However, here we assessed present versus past historical connectivity quantitatively and in a landscape explicit context. This spatial approach allows to relate population differentiation to the Pleistocene glacial cycles and the sky-island dynamics they produce in tropical mountains.

Our results support the ongoing role of tropical mountains as cradles for biodiversity by uncovering cryptic differentiation and limits to gene flow, and as museums for biodiversity by promoting long-term *in situ* persistence. Therefore, the conservation importance of tropical mountains, such as the ones of the TMVB, resides not only on its species richness *per se*, but on that landscapes like these promote both long-term population survival and further diversification.

References

Adams RP (2014) *Junipers of the world: The genus Juniperus*. Trafford Publishing.

Almeida-Leñero, L., Escamilla, M., Giménez de Azcárate, J., González-Trápaga, A., Cleff, A. M. (2007) Vegetación alpina de los volcanes Popocatépetl, Iztaccíhuatl y Nevado de Toluca. In: *Biodiversidad de la faja volcánica Trans-Mexicana* (eds Luna-Vega I, Morrone JJ, Espinosa D), pp. 179–198. Universidad Nacional Autónoma de México, Facultad de Estudios Superiores Zaragoza e Instituto de Biología.

Araújo MB, Guisan A (2006) Five (or so) challenges for species distribution modelling. *Journal of Biogeography*, **33**, 1677–1688.

Beaman JH (1962) The Timberlines of Iztaccihuatl and Popocatepetl, Mexico. *Ecology*, **43**, 377–385.

Bonner FT (2008) Juniperus L. juniper. In: *Seeds of woody plants in the United States* Agriculture Handbook. (eds Bonner FT, Karrfalt RP), pp. 607–614. USDA Forest Service.

Braconnot P, Otto-Bliesner B, Harrison S *et al.* (2007) Results of PMIP2 coupled simulations of the Mid-Holocene and Last Glacial Maximum – Part 1: experiments and large-scale features. *Clim. Past*, **3**, 261–277.

Bryson RW, García-Vázquez UO, Riddle BR (2012a) Relative roles of Neogene vicariance and Quaternary climate change on the historical diversification of bunchgrass lizards (Sceloporus scalaris group) in Mexico. *Molecular Phylogenetics and Evolution*, **62**, 447–457.

Bryson RW, García-Vázquez UO, Riddle BR (2012b) Diversification in the Mexican horned lizard Phrynosoma orbiculare across a dynamic landscape. *Molecular Phylogenetics and Evolution*, **62**, 87–96.

Bryson RW, Murphy RW, Lathrop A, Lazcano-Villareal D (2011) Evolutionary drivers of phylogeographical diversity in the highlands of Mexico: a case study of the Crotalus triseriatus species group of montane rattlesnakes. *Journal of Biogeography*, **38**, 697–710.

Caballero-Rodríguez D, Lozano-García S, Correa-Metrio A (2017) Vegetation assemblages of central Mexico through the late Quaternary: modern analogs and compositional turnover. *Journal of Vegetation Science*, doi:10.1111/jvs.12515.

Cadena CD, Kozak KH, Gómez JP *et al.* (2011) Latitude, elevational climatic zonation and speciation in New World vertebrates. *Proceedings of the Royal Society B: Biological Sciences*, rspb20110720.

Calderón de Rzedowski G, Rzedowski J (2005) *Flora Fanerogámica del Valle de México*. Instituto de Ecología A.C. y Comisión Nacional para el Conocimiento y Uso de la Biodiversidad, Pátzcuaro, Michoacán, México.

Carnaval AC, Hickerson MJ, Haddad CFB, Rodrigues MT, Moritz C (2009) Stability predicts genetic diversity in the Brazilian Atlantic forest hotspot. *Science*, **323**, 785 – 789.

Catchen J, Amores A, Hohenlohe P, Cresko W, Postlethwait JH (2011) Stacks: building and genotyping loci *de novo* from short-read sequences. *G3: Genes, Genomes, Genetics*, **1**, 171–182.

Catchen J, Hohenlohe PA, Bassham S, Amores A, Cresko WA (2013) Stacks: an analysis tool set for population genomics. *Molecular Ecology*, **22**, 3124–3140.

Csilléry K, François O, Blum MGB (2012) abc: an R package for approximate Bayesian computation (ABC). *Methods in Ecology and Evolution*, **3**, 475–479.

Devitt TJ, Devitt SEC, Hollingsworth BD, McGuire JA, Moritz C (2013) Montane refugia predict population genetic structure in the Large-blotched Ensatina salamander. *Molecular Ecology*, **22**, 1650–1665.

Dray S, Dufour A-B (2007) The ade4 package: implementing the duality diagram for ecologists. *Journal of statistical software*, **22**, 1–20.

Excoffier L, Dupanloup I, Huerta-Sánchez E, Sousa VC, Foll M (2013) Robust Demographic Inference from Genomic and SNP Data. *PLOS Genet*, **9**, e1003905.

Felsenstein J (1971) Inbreeding and Variance Effective Numbers in Populations with Overlapping Generations. *Genetics*, **68**, 581–597.

Ferrari L, Orozco-Esquivel T, Manea V, Manea M (2012) The dynamic history of the Trans-Mexican Volcanic Belt and the Mexico subduction zone. *Tectonophysics*, **522–523**, 122–149.

Fjeldså J, Bowie RCK (2008) New perspectives on the origin and diversification of Africa's forest avifauna. *African Journal of Ecology*, **46**, 235–247.

Fjeldså J, Bowie RCK, Rahbek C (2012) The Role of Mountain Ranges in the Diversification of Birds. *Annual Review of Ecology, Evolution, and Systematics*, **43**, 249–265.

Fjeldså J, Lambin E, Mertens B (1999) Correlation between endemism and local ecoclimatic stability documented by comparing Andean bird distributions and remotely sensed land surface data. *Ecography*, **22**, 63–78.

Francis JK (2004) Mahonia aquifolium (Pursh) Nutt. *Wildland shrubs of the United States and its territories: thamnic descriptions*, **1**, 461.

Graham CH, Moritz C, Williams SE (2006) Habitat history improves prediction of biodiversity in rainforest fauna. *Proceedings of the National Academy of Sciences of the United States of America*, **103**, 632–636.

Gutiérrez-Rodríguez C, Ornelas JF, Rodríguez-Gómez F (2011) Chloroplast DNA phylogeography of a distylous shrub (Palicourea padifolia, Rubiaceae) reveals past fragmentation and demographic expansion in Mexican cloud forests. *Molecular Phylogenetics and Evolution*, **61**, 603–615.

Gutenkunst RN, Hernandez RD, Williamson SH, Bustamante CD (2009) Inferring the Joint Demographic History of Multiple Populations from Multidimensional SNP Frequency Data. *PLOS Genet*, **5**, e1000695.

Hewitt GM (1996) Some genetic consequences of ice ages, and their role in divergence and speciation. *Biological Journal of the Linnean Society*, **58**, 247–276.

Hijmans RJ, Cameron SE, Parra JL, Jones PG, Jarvis A (2005) Very high resolution interpolated climate surfaces for global land areas. *International Journal of Climatology*, **25**.

Hugall A, Moritz C, Moussalli A, Stanisic J (2002) Reconciling paleodistribution models and comparative phylogeography in the Wet Tropics rainforest land snail Gnarosophia bellendenkerensis (Brazier 1875). *Proceedings of the National Academy of Sciences of the United States of America*, **99**, 6112 –6117.

Jetz W, Rahbek C (2002) Geographic range size and determinants of avian species richness. *Science*, **297**, 1548 –1551.

Jetz W, Rahbek C, Colwell RK (2004) The coincidence of rarity and richness and the potential signature of history in centres of endemism. *Ecology Letters*, **7**, 1180–1191.

Kessler M (2002) The elevational gradient of Andean plant endemism: varying influences of taxon-specific traits and topography at different taxonomic levels. *Journal of Biogeography*, **29**, 1159–1165.

Krömer T, Acebey A, Kluge J, Kessler M (2013) Effects of altitude and climate in determining elevational plant species richness patterns: A case study from Los Tuxtlas, Mexico. *Flora - Morphology, Distribution, Functional Ecology of Plants*, **208**, 197–210.

Kruckeberg AR, Rabinowitz D (1985) Biological aspects of endemism in higher plants. *Annual Review of Ecology and Systematics*, **16**, 447–479.

Lauer W (1978) Timberline studies in Central Mexico. *Arctic and Alpine Research*, **10**, 383.

Leaché AD, Palacios JA, Minin VN, Bryson RW (2013) Phylogeography of the Trans-Volcanic bunchgrass lizard (*Sceloporus bicanthalis*) across the highlands of south-eastern Mexico. *Biological Journal of the Linnean Society*, **110**, 852–865.

Lee-Yaw JA, Davidson A, McRae BH, Green DM (2009) Do landscape processes predict phylogeographic patterns in the wood frog? *Molecular Ecology*, **18**, 1863–1874.

Liaw A, Wiener M (2002) Classification and Regression by randomForest. *R News*, **2**, 18–22.

Loarie SR, Duffy PB, Hamilton H *et al.* (2009) The velocity of climate change. *Nature*, **462**, 1052–1055.

Lozano-García MS, Ortega-Guerrero B (1994) Palynological and magnetic susceptibility records of Lake Chalco, central Mexico. *Palaeogeography, Palaeoclimatology, Palaeoecology*, **109**, 177–191.

Lozano-García MS, Ortega-Guerrero B (1998) Late Quaternary environmental changes of the central part of the Basin of Mexico; correlation between Texcoco and Chalco basins. *Review of Palaeobotany and Palynology*, **99**, 77–93.

Lozano-García S, Sosa-Nájera S, Sugiura Y, Caballero M (2005) 23,000 yr of vegetation history of the Upper Lerma, a tropical high-altitude basin in Central Mexico. *Quaternary Research*, **64**, 70–82.

Lozano-García S, Vázquez-Selem L (2005) A high-elevation Holocene pollen record from Iztaccihuatl volcano, central Mexico. *The Holocene*, **15**, 329–338.

Mastretta-Yanes A, Moreno-Letelier A, Piñero D, Jorgensen TH, Emerson BC (2015a) Biodiversity in the Mexican highlands and the interaction of geology, geography and climate within the Trans-Mexican Volcanic Belt. *Journal of Biogeography*, 1586–1600.

Mastretta-Yanes A, Arrigo N, Alvarez N *et al.* (2015b) Data from: RAD sequencing, genotyping error estimation and de novo assembly optimization for population genetic inference. *Dryad Digital Repository.*, doi:10.5061/dryad.g52m3.

Mastretta-Yanes A, Arrigo N, Alvarez N *et al.* (2015c) Restriction site-associated DNA sequencing, genotyping error estimation and de novo assembly optimization for population genetic inference. *Molecular Ecology Resources*, **15**, 28–41.

Mastretta-Yanes, A. (2014). *Landscape genomics of tropical high altitude plant species* (doctoral thesis). University of East Anglia. Retrieved from https://ueaeprints.uea.ac.uk/52157/

Mastretta-Yanes A, Zamudio S, Jorgensen TH *et al.* (2014) Gene duplication, population genomics and species-level differentiation within a tropical mountain shrub. *Genome Biology and Evolution*, **6**, 2611-2624.

McCormack JE, Peterson AT, Bonaccorso E, Smith TB (2008) Speciation in the highlands of Mexico: genetic and phenotypic divergence in the Mexican jay (*Aphelocoma ultramarina*). *Molecular Ecology*, **17**, 2505–2521.

McRae BH (2006) Isolation by resistance. *Evolution*, **60**, 1551-1561.

McRae BH, Beier P (2007) Circuit theory predicts gene flow in plant and animal populations. *Proceedings of the National Academy of Sciences*, **104**, 19885 –19890.

McRae BH, Dickson BG, Keitt TH, Shah VB (2008) Using circuit theory to model connectivity in ecology, evolution, and conservation. *Ecology*, **89**, 2712–2724.

Moore JA, Tallmon DA, Nielsen J, Pyare S (2011) Effects of the landscape on boreal toad gene flow: does the pattern–process relationship hold true across distinct landscapes at the northern range margin? *Molecular Ecology*, **20**, 4858–4869.

Myers N, Mittermeier RA, Mittermeier CG, da Fonseca GAB, Kent J (2000) Biodiversity hotspots for conservation priorities. *Nature*, **403**, 853–858.

Ohlemüller R, Anderson BJ, Araújo MB *et al.* (2008) The coincidence of climatic and species rarity: high risk to small-range species from climate change. *Biology Letters*, **4**, 568–572.

Oksanen J, Blanchet FG, Friendly M et al. (2016) vegan: Community Ecology Package. http://CRAN.R-project.org/package=vegan

Ornelas JF, Ruiz-Sánchez E, Sosa V (2010) Phylogeography of *Podocarpus matudae* (Podocarpaceae): pre-Quaternary relicts in northern Mesoamerican cloud forests. *Journal of Biogeography*, **37**, 2384–2396.

Ornelas JF, Sosa V, Soltis DE *et al.* (2013) Comparative phylogeographic analyses illustrate the complex evolutionary history of threatened cloud forests of Northern Mesoamerica. *PLoS ONE*, **8**, e56283.

Orsini L, Vanoverbeke J, Swillen I, Mergeay J, De Meester L (2013) Drivers of population genetic differentiation in the wild: isolation by dispersal limitation, isolation by adaptation and isolation by colonization. *Molecular Ecology*, **22**, 5983-5999.

Päckert M, Martens J, Sun Y-H *et al.* (2012) Horizontal and elevational phylogeographic patterns of Himalayan and Southeast Asian forest passerines (Aves: Passeriformes). *Journal of Biogeography*, **39**, 556–573.

Paradis E, Claude J, Strimmer K (2004) APE: Analyses of Phylogenetics and Evolution in R language. *Bioinformatics*, **20**, 289–290.

Parchman TL, Gompert Z, Mudge J *et al.* (2012) Genome-wide association genetics of an adaptive trait in lodgepole pine. *Molecular Ecology*, **21**, 2991–3005.

Parra-Olea G, Windfield JC, Velo-Antón G, Zamudio KR (2012) Isolation in habitat refugia promotes rapid diversification in a montane tropical salamander. *Journal of Biogeography*, **39**, 353–370.

Peterson BK, Weber JN, Kay EH, Fisher HS, Hoekstra HE (2012) double digest radseq: an inexpensive method for de novo SNP discovery and genotyping in model and non-model species. *PLoS ONE*, **7**, e37135.

Peterson PDJ (2003) The Common Barberry: The Past and Present Situation in Minnesota and the Risk of Wheat Stem Rust Epidemics. PhD Thesis. North Carolina State University.

Prates I, Xue AT, Brown JL *et al.* (2016) Inferring responses to climate dynamics from historical demography in neotropical forest lizards. *Proceedings of the National Academy of Sciences*, **113**, 7978–7985.

Phillips SJ, Anderson RP, Schapire RE (2006) Maximum entropy modeling of species geographic distributions. *Ecological Modelling*, **190**, 231–259.

Rahbek C, Gotelli NJ, Colwell RK *et al.* (2007) Predicting continental-scale patterns of bird species richness with spatially explicit models. *Proceedings of the Royal Society B: Biological Sciences*, **274**, 165–174.

R. Core Team (2012) *R: A Language and Environment for Statistical Computing*. R Foundation for Statistical Computing, Vienna, Austria.

Roberts DR, Hamann A (2012) Method selection for species distribution modelling: are temporally or spatially independent evaluations necessary? *Ecography*, **35**, 792–802.

Rounsaville TJ, Ranney TG (2010) Ploidy levels and genome sizes of *Berberis* L. and *Mahonia* nutt. species, hybrids, and cultivars. *HortScience*, **45**, 1029–1033.

Rousset F (1997) Genetic differentiation and estimation of gene flow from F-statistics under isolation by distance. *Genetics*, **145**, 1219–1228.

Rzedowski J (1978) *Vegetación de México*. Limusa, México.

Sandel B, Arge L, Dalsgaard B *et al.* (2011) The influence of late Quaternary climate-change velocity on species endemism. *Science*, **334**, 660 –664.

Smith BT, McCormack JE, Cuervo AM *et al.* (2014) The drivers of tropical speciation. *Nature*, doi: 10.1038/nature13687

Stewart JR, Lister AM, Barnes I, Dalén L (2010) Refugia revisited: individualistic responses of species in space and time. *Proceedings of the Royal Society B: Biological Sciences*, **277**, 661–671.

Toledo V (1982) Pleistocene changes of vegetation in tropical Mexico. In: *Biological diversification in the tropics* (ed Prance GT), pp. 93–111. Columbia University Press, New York.

Vázquez-Selem L, Heine K (2011) Late Quaternary Glaciation in Mexico. In: *Quaternary Glaciations - Extent and Chronology - A Closer Look* (eds Ehlers J, Gibbard PL, Hughes P), pp. 849–861. Elsevier.

Wang IJ (2013) Examining the full effects of landscape heterogeneity on spatial genetic variation: a multiple matrix regression approach for quantifying geographic and ecological isolation. *Evolution*, **67**, 3403–3411.

Webb T, Bartlein PJ (1992) Global changes during the last 3 million years: climatic controls and biotic responses. *Annual Review of Ecology and Systematics*, **23**, 141–173.

Weir JT (2009) Implications of genetic differentiation in Neotropical montane forest birds. *Annals of the Missouri Botanical Garden*, **96**, 410–433.

Wickham H, Chang W (2013) *ggplot2: An implementation of the Grammar of Graphics*. v. 0.9.3.1. CRAN repository.

Xue AT, Hickerson MJ (2015) The aggregate site frequency spectrum (aSFS) for comparative population genomic inference. *Molecular Ecology*, **24**, 6223–6240.

Xue AT, Hickerson MJ (2017) Multi-DICE: R package for comparative population genomic inference under multi-taxa hierarchical co-demographic models. *Molecular Ecology Resources.* 1–13. doi:10.1111/1755-0998.12686

Zheng, X., Levine, D., Shen, J., Gogarten, S. M., Laurie, C., & Weir, B. S. (2012). A high-performance computing toolset for relatedness and principal component analysis of SNP data. *Bioinformatics*, *28*(24), 3326–3328. doi:10.1093/bioinformatics/bts606

Zonneveld BJM (2012) Conifer genome sizes of 172 species, covering 64 of 67 genera, range from 8 to 72 picogram. *Nordic Journal of Botany*.

Data Accessibility

This project has been deposited at Dryad Repository under the accession doi:10.5061/dryad.f7248. The repository includes lab protocol, species occurrence data, spatial data, genetic data in plink format and the scripts used for all analyses. Raw RADseq data is at the Sequence Read Archive (SRA) accession SRP035472 for *Berberis* and SRP125588 for *Juniperus.*

Author Contributions

AMY, DP, THJ and BCE conceived and designed the study. AMY performed fieldwork and laboratory work, assembled the RAD data and made all analyses, except for the aSFS and the ecosystem distribution modelling. ATX performed the aSFS analyses. AML

performed the ecosystem distribution modelling. NA and THJ supervised lab work and preliminary analyses. AMY, DP and BCE lead manuscript writing. All authors contributed to the discussion and manuscript writing.

Table 1. Summary population genetic statistics for *B. alpina* and *J. monticola*

Pop. ID	*Ns*	*N*	Priv.	Sites	P	H_{obs}	π	F_{IS}
B. alpina								
Pe	8	6.11	1101	2183	0.9108	0.1234	0.1395	0.0374
Tl	6	4.76	332	1557	0.9383	0.0917	0.1020	0.0235
Ma	8	6.42	503	1743	0.9338	0.0967	0.1060	0.0219
Iz	10	8.03	375	1708	0.9404	0.0924	0.0951	0.0141
Aj	10	8.54	477	1892	0.9357	0.1006	0.1025	0.0073
To	8	6.31	326	1376	0.9449	0.0908	0.0883	0.0004
J. monticola								
Ch	8	7.03	608	2691	0.9421	0.0689	0.0936	0.0650
Pe	5	4.04	206	1569	0.9549	0.0577	0.0741	0.0326
Ci	10	9.06	176	2189	0.9515	0.0583	0.0757	0.0465
Ne	10	8.70	177	2236	0.9522	0.0582	0.0756	0.0460
Ma	9	7.27	175	1842	0.9543	0.0487	0.0713	0.0564
Tl	10	8.81	324	2646	0.9461	0.0661	0.0860	0.0554
Iz	8	6.64	265	2337	0.9482	0.0651	0.0844	0.0492
Pp	8	7.00	208	2190	0.9497	0.0587	0.0804	0.0553
Aj	7	4.90	194	1812	0.9515	0.0505	0.0785	0.0622
To	8	6.13	154	1673	0.9549	0.0495	0.0706	0.0491
Bl	9	7.62	327	2260	0.9486	0.0626	0.0808	0.0468
Ta	10	8.40	431	2298	0.9467	0.0594	0.0826	0.0580
Co	8	5.37	309	1994	0.9477	0.0508	0.0849	0.0777

Results include only nucleotide positions that are polymorphic in at least one population. The first column shows the number of individuals per population that were used for the analysis (Ns). Next are the average number of individuals genotyped at each locus (N), the number of variable sites unique to each population (i.e. private alleles, Priv.), the number of polymorphic nucleotide sites for that population (Sites), the average frequency of the major allele (P), the average observed heterozygosity per locus (H_{obs}), the average nucleotide diversity (π), and the average Wright's inbreeding coefficient (F_{IS}). Populations are ordered East to West, top to bottom. Population IDs as in Fig. 1.

Table 2. Isolation by resistance

Surface	*B. alpina* r		Pt r		*J. monticola* all pops. r		Pt r		*J. monticola* excluding Co & Ta r		Pt r	
present	0.787	**	0.059	NS	0.469	*	-0.034	NS	0.662	***	0.406	**
ccsm	0.662	*	-0.061	NS	0.402	*	-0.140	NS	0.686	***	0.453	**
miroc	0.792	**	0.218	NS	0.430	*	-0.129	NS	0.675	***	0.427	**
flat	0.881	**	-	-	0.499	*	-	-	0.579	***	-	-
1,800	0.888	**	0.244	NS	0.327	NS	-0.374	NS	0.575	***	0.087	NS
2,000	0.893	***	0.307	NS	0.299	NS	-0.376	NS	0.566	***	0.052	NS
2,300	0.827	**	-0.311	NS	0.319	NS	-0.343	NS	0.555	***	0.022	NS
2,500	0.901	**	0.417	NS	0.384	NS	-0.285	NS	0.530	**	0.005	NS
2,700	0.929	**	0.620	*	0.443	*	-0.159	NS	0.550	***	0.068	NS
3,000	0.940	**	0.717	*	0.374	*	-0.184	NS	0.331	NS	-0.188	NS
3,300	0.905	**	0.435	NS	0.389	*	-0.180	NS	0.353	NS	-0.230	NS
3,500	0.833	**	0.023	NS	0.386	*	-0.149	NS	0.34	NS	-0.272	NS
4,000	0.681	*	-0.017	NS	0.378	*	-0.201	NS	0.335	NS	-0.249	NS

Associations between genetic differentiation (linearized F_{ST}, see main text) and pairwise effective distances at different surfaces (see Fig. 2 for an explanation of these). Mantel test *r* value (*r*) and Partial Mantel test *r* value (Pt *r*) are reported for each species. Significance codes are as follows: < 0.001 '***', <0.01 '**', < 0.05 '*', and not significant 'NS'. Underlined cells correspond to the surface with the highest prediction value for each taxon.

Table 3. Proportion of populations in synchrony and number of synchronous pulses.

Estimation method	ζ			ψ		
	res	*r*	*rmse*	res	*r*	*rmse*
hRF Hyperparameter Estimation	0.821	0.613	0.229	1.81	0.784	0.70
hABC Hyperparameter Estimation - Median	0.929	0.610	0.236	1.00	0.761	0.92
hABC Hyperparameter Estimation - Mode	0.999	0.561	0.303	1.00	0.619	1.05

Results for the downprojection to four individuals, see Table S2.4 for results with the downprojection to five. ζ: proportion of populations in synchrony (considering both species together). ψ: number of synchronous pulses. For ζ and ψ, the three columns show the resulting estimation (res), and the cross-validation accuracy check based on the correlation (*r*) and the root mean squared error (*rmse*) between the simulated true values and the estimated values.
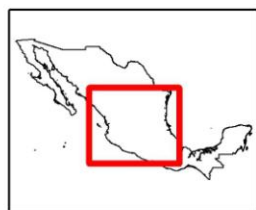
Elevation (masl)

- ▢ 0 to <3,000
- ▢ 3,000 to > 5,000

▲ **Surveyed mountains**

SMOr
Pt: Cerro Potosí   **Mt** La Marta

AS
Za: Cerro Zamorano

TMVB

Ch El Chico	**Pp** Popocatépetl
Pe Cofre de Perote	**Aj** Ajusco
Ci Citaltépetl	**To** Nevado de Toluca
Ne Sierra Negra	**Bl** Cerro Blanco
Ma La Malinche	**An** Cerro Sn Andrés
Tl Tláloc	**Ta** Tancítaro
Iz Iztaccíhuatl	**Co** Nevado de Colima

Tropic of Cancer

A)

bio1- Annual mean temperature
bio2- Mean diurnal range
bio3- Isothermality (bio2/bio7)*
bio4- Temperature seasonality
bio5- Max. temp. warmest quarter
bio6- Min. temp. coldest month
bio7- Temperature annual range*
bio8- Mean Temp. wettest quarter*
bio9- Mean temp. driest quarter
bio10- Mean temp. warmest quarter
bio11- Mean temp. coldest quarter
bio12- Annual precipitation
bio13- Precipitation wettest month
bio14- Precipitation driest month
bio15- Precipitation seasonality*
bio16- Precipitation wettest quarter
bio17- Precipitation driest quarter
bio18- Precipitation warmest quarter
bio19- Precipitation coldest quarter*

B)

a)

b)

c)